

Gelation-Induced Phase Separation of Poly(vinyl alcohol) in Mixed Solvents of Dimethyl Sulfoxide and Water

Nobuaki Takahashi,[†] Toshiji Kanaya,^{*,‡} Koji Nishida,[‡] and Keisuke Kaji[‡]

J-PARC Center, Japan Atomic Energy Agency, Shirakatashirane 2-4, Tokai, Naka, Ibaraki 319-1195, Japan, and Institute for Chemical Research, Kyoto University, Gokasho, Uji, Kyoto 611-0011, Japan

Received June 6, 2007; Revised Manuscript Received September 13, 2007

ABSTRACT: Time-resolved light-scattering measurements have been performed on poly(vinyl alcohol) (PVA) in mixed solvents of dimethyl sulfoxide (DMSO) and water with various mixing ratios after quenching from 100 to 25 °C to examine the physical gelation process. A broad scattering peak characteristic of phase separation appeared in the light-scattering profiles after a certain incubation time (t_m) and the peak position (Q_m) moved to higher Q with annealing time. The results contradict the theoretical predictions and experimental observations for usual phase separation systems, suggesting the effects of gelation (or network formation) on the phase separation. The growth kinetics significantly depend on the mixing ratio of DMSO and water, showing that the solvent quality is also a factor to affect the phase separation kinetics during the physical gelation process. The unusual phase separation kinetics is discussed in terms of gelation-induced phase separation.

1. Introduction

Poly(vinyl alcohol) (PVA) is one of the most interesting polymers, because it is water-soluble and biocompatible. Hence, PVA is used in various ways in our daily life. It is well-known that PVA gels physically in various solvents, such as water, dimethyl sulfoxide (DMSO), and polyethylene glycol (PEG), upon cooling. We have so far extensively studied formation mechanism,^{1–3} static structure,^{4–6} dynamical behavior,⁷ and gelation kinetics⁸ of PVA gels in DMSO/water mixed solvents. It was found^{4,8} that microcrystallites, which are formed by quenching the PVA solution, work as cross-linking points of the physical gel. Depending on both the quenching temperature^{9,10} and solvent composition,¹¹ the formed gels show a variety of macroscopic appearances, namely, transparent, translucent, and opaque. Since PVA solution has an upper critical solution temperature (UCST)-type phase diagram, the phase separation is often concomitant with the physical gelation^{2,5,6} upon cooling. When the phase separation precedes the network formation to give a bicontinuous structure of polymer-rich and polymer-poor phases and the network formation occurs in the polymer-rich phase, the resultant gel is opaque. The origin of the opaqueness is ascribed to liquid–liquid phase separation. Similar phenomena were reported for concentrated solutions of poly(γ -benzyl- α ,L-glutamate) (PBLG) in *N,N*-dimethylformamide containing a small amount of water.¹² In order to elucidate the phase separation mechanism as well as the gelation mechanism, Takeshita et al.² have conducted time-resolved light-scattering (LS) measurements on PVA solutions in the DMSO/water mixed solvent with a volume fraction of DMSO, ϕ_{DMSO} , of 0.6 after a temperature jump from 100 to 25 °C. The scattering profile showed a maximum at a position Q_m , which scarcely moved with time, and the maximum intensity (I_m) increased exponentially with annealing time. These results are well-described by the theory for the initial stage of spinodal decomposition (SD)-type phase separation reported by Cahn and Hilliard.^{13–15} On the basis of the results, they proposed a

structure formation mechanism for the PVA gel in DMSO/water with $\phi_{\text{DMSO}} = 0.6$. When quenching the PVA solution to 25 °C, it stayed in the SD region or an unstable region, and hence SD-type liquid–liquid phase separation proceeded before gelation (or network formation). After the solution is phase-separated into bicontinuous polymer-rich and polymer-poor regions, network formation due to crystallization occurs in the bicontinuous polymer-rich phase, resulting in the macroscopic opaque PVA gel. This explanation seems very reasonable and well explains the observed results.

Recently, we have examined PVA solutions in DMSO/water mixed solvents to investigate effects of solvent composition on both gelation and phase separation rates and have found both of them significantly depended on the solvent composition.¹¹ In pure DMSO and water, PVA gelation and phase separation rates are extremely slow, while they increase in mixed solvent and show a maximum at $\phi_{\text{DMSO}} = 0.6$, meaning that the mixed solvent with $\phi_{\text{DMSO}} = 0.6$ is the poorest solvent for PVA. This result can be understood in terms of the co-nonsolvency effect.¹⁶ Of further interest is how the solvent quality affects the detailed manner of phase separation and gelation. Consequently, in this work, we have performed time-resolved LS measurements on PVA solutions with various solvent compositions.

2. Experimental Section

Fully saponified atactic PVA with a number-average degree of polymerization $\text{DP}_n = 1730$ was used in this work. The molecular weight distribution M_w/M_n is 1.97, where M_w and M_n are weight- and number-average molecular weights, respectively. The details of the characterization of this sample were reported elsewhere.⁹ The solvents used for the experiments were mixtures of dimethyl sulfoxide (DMSO) and water with $\phi_{\text{DMSO}} = 0.30, 0.40, 0.50, 0.60, 0.68, 0.72, 0.76$, and 0.80 .

A given amount of PVA was dissolved in a solvent at about 130 °C in an autoclave to be homogenized in a glass tube, and then the solution was filtered through a 0.45 μm Millipore filter in a dust-free cylindrical Pyrex cell with a diameter of 10 mm. Just before the measurements, the samples in the cell were again homogenized at 100 °C for about 30 min and quenched to 25 °C for gelation. PVA concentration (C_p) was 5 g/dL for the measurements.

* Corresponding author. Tel +81-774-38-3141; Fax +81-774-38-3146; e-mail kanaya@scl.kyoto-u.ac.jp.

[†] Japan Atomic Energy Agency.

[‡] Kyoto University.

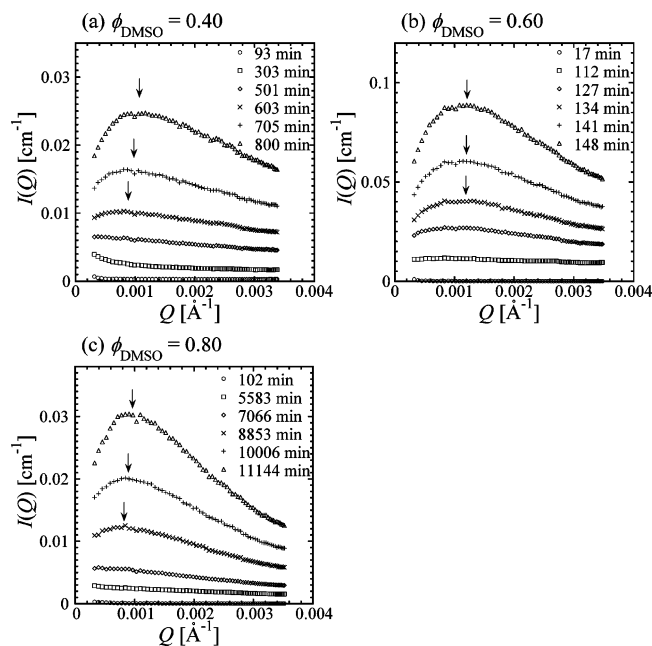


Figure 1. Time evolutions of LS profiles of PVA solution in mixtures of DMSO and water with $C_p = 5$ g/dL after quenching from 100 to 25 °C. The volume fractions of DMSO, ϕ_{DMSO} , are (a) 0.4, (b) 0.6, and (c) 0.8.

Light-scattering (LS) measurements were carried out with a System 4700 of Malvern Instruments Inc. using Ar⁺ laser ($\lambda = 488$ nm, 75 mW) as a light source. The scattering vector, $Q (=4n\pi \sin\theta/\lambda)$, with n being the refractive index, covers a range between 3.2×10^{-4} and $3.6 \times 10^{-3} \text{ Å}^{-1}$. The absolute intensity (Rayleigh ratio) was calculated using toluene as a standard to be $R_{\text{tol}} = 39.6 \times 10^{-6} \text{ cm}^{-1}$ for $\lambda = 488$ nm at $T = 25$ °C.¹⁷ In order to reduce the effect of speckle, measurements were performed by rotating the sample cell at a frequency of about 10 rpm.² Time-resolved LS measurements were started just after transferring the solution at 100 °C to a sample cell holder that had been kept at 25 °C. The scattering intensity $I(Q)$ was corrected for the transmittance of the laser beam with wavelength of 488 nm.

3. Results and Discussion

Time evolutions of LS profiles are shown for $\phi_{\text{DMSO}} = 0.4$, 0.6, and 0.8 in Figure 1, parts a, b, and c, respectively. In all DMSO fractions, a broad peak characteristic of phase separation appears in the LS profiles after a certain incubation time (t_m) and grows in intensity with annealing time. Apparently, large differences are not found in the time evolutions of LS profiles for $\phi_{\text{DMSO}} = 0.4$, 0.6, and 0.8. In order to examine the phase separation kinetics, the peak position Q_m and the peak intensity are plotted against the annealing time for $\phi_{\text{DMSO}} = 0.4$, 0.6, and 0.8 in Figure 2, parts a, b, and c, respectively, where the incubation time t_m of the peak as well as macroscopic gelation time (t_{gel}) determined by the tilting method are indicated by dotted and dashed lines, respectively. The incubation time t_m and macroscopic gelation time t_{gel} strongly depend on the DMSO fraction ϕ_{DMSO} . To see the effect of the solvent composition, the incubation time t_m and macroscopic gelation time t_{gel} are plotted against DMSO fraction ϕ_{DMSO} in Figure 3. Both of them are extremely short at around $\phi_{\text{DMSO}} = 0.6$, showing that the mixed solvent with $\phi_{\text{DMSO}} = 0.6$ is the poorest solvent for PVA.

In this work, we again performed LS measurements on PVA in DMSO/water mixed solvent with $\phi_{\text{DMSO}} = 0.6$. As reported in a previous paper² and seen in Figures 1b and 2b, the peak position Q_m almost stays constant at $Q = 1.2 \times 10^{-3} \text{ Å}^{-1}$, and the peak intensity increases exponentially with annealing time

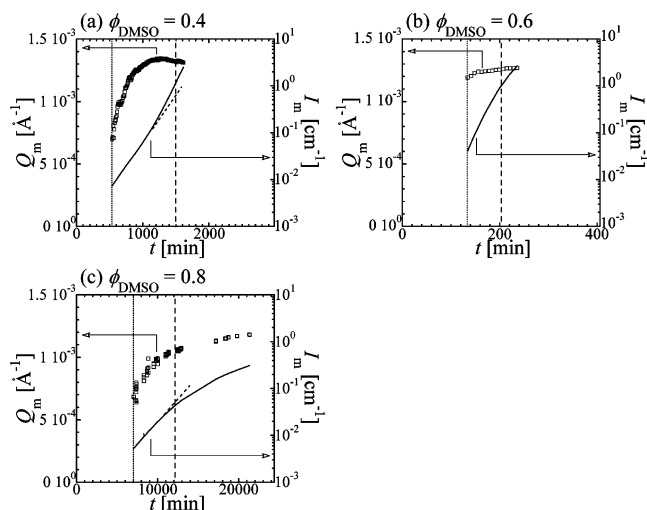


Figure 2. Time evolutions of the peak position Q_m (open square, left axis with linear scale) and intensity at peak position I_m (solid line, right axis with logarithmic scale). The dotted and broken vertical lines indicate t_m and t_{gel} , respectively. The volume fractions of DMSO, ϕ_{DMSO} , are (a) 0.4, (b) 0.6, and (c) 0.8.

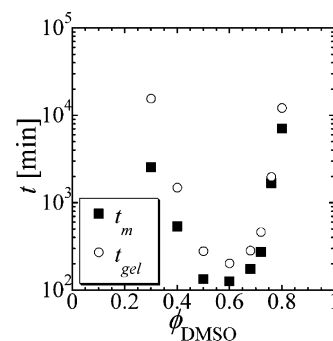


Figure 3. Solvent composition dependences of onset time of peak appearance on LS profile, t_m (■), and gelation time, t_{gel} (○).

before the macroscopic gelation. The results completely agree with the theoretical prediction for the initial stage of SD-type phase separation by Chan–Hilliard,^{13–15} concluding that the SD-type phase separation occurs before the gelation, resulting in bicontinuous polymer-rich and polymer-poor phases. The cross-linking points between PVA chains due to crystallization are mainly formed in the bicontinuous polymer-rich phase, leading to macroscopic gelation. This is a scenario for the formation of opaque PVA gels in DMSO/water mixed solvent with $\phi_{\text{DMSO}} = 0.6$.² It is noted that the scattering profile has no peak in the early stage before about 120 min, although the intensity increases exponentially with time. According to the theory,^{13–15} the peak due to the SD-type phase separation must appear just after quenching into the SD region, because the SD region is unstable. The results do not agree with the theory. In a previous paper,² we considered that the contradiction was caused by the fluctuations due to the microgel formation: the cross-linking among PVA chains occurred simultaneously with phase separation to form microgels, and the fluctuations probably hid the broad peak due to the SD-type phase separation. This problem will be again discussed later.

The phase separation kinetics becomes very different from that of $\phi_{\text{DMSO}} = 0.6$ when the fraction of DMSO departs from 0.6, as seen in Figures 1a,c and 2a,c. As the solvent composition is going away from $\phi_{\text{DMSO}} = 0.6$, the macroscopic gelation time t_{gel} becomes longer, as seen in Figure 3, showing that the mixed solvent becomes better for PVA. These phenomena can be understood as co-nonsolvency effects.¹¹ In addition to the

slowing down in gelation rate, we found that the incubation time t_m of the scattering peak is very long compared with that for $\phi_{\text{DMSO}} = 0.6$ (for example, $t_m = 500$ and 6800 min for $\phi_{\text{DMSO}} = 0.4$ and 0.8, respectively; see also Figure 3), although the scattering intensity increases with annealing time before emergence of the peak. Furthermore, the peak position Q_m shifts to higher Q with annealing time. These results cannot be understood as normal SD-type phase separation. According to the theories,^{13–15} which were confirmed in many experiments,¹⁸ concentration fluctuations due to SD-type phase separation must start spontaneously after temperature jump into SD-region, because the SD-region is an unstable region. The theory also predicts that the peak position Q_m , which correspond to the inverse of the characteristic length of phase separation Λ ($=2\pi/Q_m$), remains constant in the early stage of SD-type phase separation and shifts to lower Q in the late stage according to a power law, keeping the self-similarity, due to coalescence of phase-separated domains. The present findings on the kinetics for PVA solutions in mixed solvents except for $\phi_{\text{DMSO}} = 0.6$ are completely different from normal SD-type phase separation. How can we understand the unusual results? One of the keys to solve the problem is that phase separation occurs simultaneously with gelation (or network formation); hence, we have to consider the relation between the phase separation rate and gelation rate. We also have to consider the solvent quality, because the rate of gelation, as well as phase separation, depends on the solvent quality. These suggest that the most important point is that the phase diagram (binodal and spinodal curves) depends on the solvent quality as well as molecular weight, which increases as the cross-linking reaction proceeds.

As mentioned above, the scattering peak is observed after a certain incubation time t_m , even for $\phi_{\text{DMSO}} = 0.6$. In the previous paper we considered that the peak was hidden by the fluctuations due to the formation of cross-linking points. However, the present observations for various DMSO compositions cannot be explained only by the effect of the fluctuations, suggesting another effect of the cross-linking reaction. PVA solutions in mixed solvent of DMSO and water have UCST-type phase diagrams. When cross-linking reactions proceed with annealing time, molecular weight increases, resulting in the upward shift (or high-temperature shift) of the phase diagram with time. This situation is very similar to polymerization-induced phase separation.¹⁹ We will apply this concept to the phase separation process of PVA solution in DMSO/water mixed solvents with various mixing ratios. Before going to the PVA gels, we will briefly explain the concept of polymerization-induced phase separation.

3.1. Polymerization-Induced Phase Separation. The polymerization-induced phase separation (PIPS) concept was reported about 2 decades ago for reactive binary polymer blends.^{20–22} The basic concept can be easily explained using schematic phase diagram presented in Figure 4. This is a temperature (T)–fraction (ϕ) phase diagram, and the bold and dotted lines indicate binodal and spinodal lines, respectively. We consider an A/B binary system with a cross-linker of component A having a UCST-type phase diagram (PD₁). It is assumed that the system is in a stable state at a given quenching temperature (T_q), denoted by a filled circle in the figure. When cross-linking reaction (polymerization) of component A occurs, the phase diagram shifts upward and leftward, for instance, PD₁ \rightarrow PD₂ \rightarrow PD₃. We now consider an A/B blend with a given composition ϕ_A at a quenching temperature T_q in the phase diagram. In the initial stage, this A/B blend is in one phase region. When the phase diagram reaches to PD₂, the A/B blend

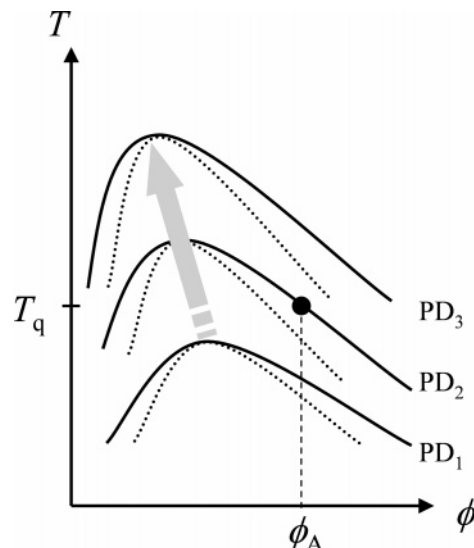


Figure 4. Schematic temperature–fraction phase diagram of an A/B binary polymer mixture. The bold and dotted lines indicate binodal and spinodal lines, respectively. The coexisting curve progressively shifts from PD₁ toward PD₃ via PD₂ in terms of polymerization of component A.

(filled circle) intersects the binodal line, resulting in a nucleation and growth (NG)-type phase separation. The polymerization reaction of component A progresses; moreover, this A/B blend with ϕ_A (filled circle) goes into the spinodal region (PD₃). This is the basic idea of PIPS, and it is noted that SD-type phase separation occurs always after getting through the metastable region. Because the critical point of phase diagram shifts upward and leftward (to the lower ϕ_A side), PIPS proceeds at an off-critical point in most cases. Thus, this pattern of SD is especially called nucleation-initiated spinodal decomposition (NISD). Within the PIPS concept, some experimental and numerical simulation works have been performed,^{23,19} revealing that a scattering peak appeared after a certain incubation time t_m and shifted to higher Q with the annealing time. These observations are qualitatively very similar to our observations in PVA gels in DMSO/water mixed solvents.

3.2. Gelation-Induced Phase Separation. Gelation of the PVA solution occurs in all solvent compositions at 25 °C,¹¹ and hence it is obvious that the cross-linking reaction proceeds before and/or during phase separation at 25 °C whether the PVA solution is in the one-phase or two-phase region, depending on the solvent quality or the mixing ratio of DMSO and water. If the solution is in the one-phase region, just after the quenching to 25 °C PIPS may occur when the cross-linking reaction proceeds. Even if the solution is in the two-phase region after quenching, the cross-linking reaction (or increase in molecular weight) affects the phase separation kinetics. In this section, we consider the effects of the cross-linking reaction on the phase separation based on the PIPS concept.

For phase separation in polymer solutions, the Flory–Huggins equation based on the combinatorial lattice model is often employed, and the free energy of mixing is given by²⁴

$$g(\phi_A) = \frac{k_B T}{v} \left\{ \frac{\phi_A}{N_A} \ln \phi_A + (1 - \phi_A) \ln(1 - \phi_A) + \chi \phi_A (1 - \phi_A) \right\} \quad (1)$$

where k_B is Boltzmann's constant, T is the absolute temperature, v is the volume of a cell or segment, ϕ_A is the polymer volume

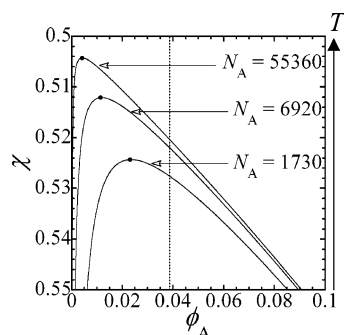


Figure 5. Spinodal lines χ_{sp} of PVA solution with various degree of polymerization, N_A , such as 1730, 6920, and 55360, are shown in the χ - ϕ phase diagram. The interaction parameter χ is inversely proportional to temperature T . The closed circles indicate critical points of corresponding spinodal lines. The dotted vertical line is corresponding to the polymer volume fraction, $C_p = 5$ g/dL.

fraction, and χ is Flory's interaction parameter. N_A is the degree of polymerization of PVA. In eq 1, we do not take into account the elasticity of the gel network, because we deal with the very early state of gelation. In addition, we also neglect the solid-liquid transition due to crystallite formation, because the amount is very small. In a strict sense, the PVA solution was a ternary system consisting of PVA and a mixed solvent of DMSO and water. We assume that it is simply treated as a binary system of polymer and mixture solvent, because no specific interactions were observed in the present fraction range. An average degree of polymerization of PVA ($=N_A$) is initially 1730. The spinodal lines χ_{sp} are calculated for various values of N_A (≥ 1730) as a function of PVA volume fraction ϕ_A and shown in Figure 5. The vertical axis (χ) corresponds to the inverse of temperature T , i.e., higher T for smaller χ . The calculated phase diagram is asymmetric, because N_A is much larger than that of the solvent N_B . The spinodal line χ_{sp} and the critical point respectively move upward and leftward as the degree of polymerization N_A increases. This is qualitatively very similar to the shift in PIPS shown in Figure 4, indicating that PIPS could occur even in the PVA solutions when the cross-linking reaction proceeds. In this paper, it is termed gelation-induced phase separation (GIPS) hereafter. The concentration of PVA in this experiment, $C_p = 5$ g/dL, is shown by a dotted vertical line in Figure 5, which corresponds to $\phi_A = 0.38$ and is larger than the critical fraction $\phi_A = 0.28$. This fact indicates that, when the cross-linking reaction proceeds and the molecular weight increases, the GIPS always occurs in the off-critical region. In other words, the phase separation initiates in the metastable nucleation and growth region (the binodal region) and then comes into the unstable spinodal decomposition region, which is often termed nucleation-initiated spinodal decomposition (NISD).^{19,25} In the light-scattering experiments on the phase separation processes of the PVA solutions in Figure 1, we observed the incubation time t_m before the appearance of a scattering peak for all solvent compositions. If the solution was quenched into the SD region, a scattering peak would be observed immediately after quenching, but we did not see it, even for the poorest solvent with $\phi_{DMSO} = 0.6$. This suggests that the solution was quenched into the one-phase region or the metastable NG region (not in the SD region). According to the scenario, the incubation time t_m can be considered as the residential time of the system staying in the stable or metastable region. Before t_m , we observed the increase of the scattering intensity without showing a peak. In the metastable NG region, the droplet nuclei are generated through NG-type phase separation mechanism before the SD-type phase separation starts. The growth in the scattering

intensity before t_m may be assigned to the fluctuations due to the nucleation. Note that the fluctuations due to the microgel formation could be also expected, even in the one-phase region. In the previous paper,² we considered that the solution with $\phi_{DMSO} = 0.6$ was quenched into the SD region, but the fluctuations due to the microgel formation hid the SD peak in the LS profile. However, the interpretation by the GIPS concept is more plausible, because it explains the observed results more systematically.

As the cross-linking reaction proceeds further, the solution comes into the unstable SD region, in which concentration fluctuations with a characteristic wavelength (Λ) are enhanced to give a scattering peak at $Q_m = 2\pi/\Lambda$. We have assigned the incubation time t_m to a time at which the solution comes into the SD region. As shown in Figure 2, the initial scattering peak position Q_m for the 60/40 solution is the highest in all solvent compositions and shifts to low Q value when apart from 60/40 at the lower and higher solvent ratios. It is known that the peak position at the initial stage of phase separation in the SD region is given by

$$Q_m = \frac{1}{l} \left| 3 \frac{T_s - T}{T_s} \right|^{1/2} \quad (2)$$

under the mean field approximation,²⁶ where $T_s - T$ is the distance between the spinodal temperature and the annealing temperature (or the quenching depth) and l is a range of molecular interaction. This equation shows that the deeper the quenching depth, the higher the Q_m value. In the present experiment, at 25 °C the quenching depth is determined by the temperature at which the phase diagram exists. In other words, the quenching depth becomes larger as the solvent becomes poorer. In fact, the deepest quenching depth is realized at $\phi_{DMSO} = 0.6$, which is the poorest solvent. This is the reason why the scattering peak is observed at the highest Q_m for the solution with $\phi_{DMSO} = 0.6$.

As the annealing time proceeds, the peak position gradually shifts to higher Q values for all the solvent compositions. For the solution with $\phi_{DMSO} = 0.6$, the peak is almost independent of the annealing time, but strictly speaking, it slightly shifts to the higher value. Such higher Q shift is unusual in the normal isothermal SD-type phase separation. As shown in Figure 5, the phase diagram gradually shifts upward and leftward with the cross-linking reaction proceeds, meaning that the quenching depth increases with annealing time. According to the eq 2, the peak position Q_m gradually shifts to higher Q as the quenching depth increases for the early stage of the SD-type phase separation. This must be a cause for the high Q shift of the peak position with the annealing time, at least in the early stage of SD-type phase separation. In the late stage of usual isothermal phase separation, it is well known that the coalescence of the phase-separated domains proceeds to reduce the interfacial energy, leading to an increase of the average domain size, and the increase in the average domain size is observed in scattering experiments as a peak shift to low Q according to a power law $Q_m \sim t^{-a}$.²⁷ In the GIPS process, it is not known theoretically how the effects of the coalescence appears. In the simulation study of PIPS,¹⁹ however, it was shown that the time evolution of the peak position Q_m could be described by

$$Q_m \sim (t - t_m)^n \quad (3)$$

According to the simulation study, the exponent n was between -1 and $1/2$. In the former and latter limits, the coarsening effect and the supercooling effect were dominant, respectively. In

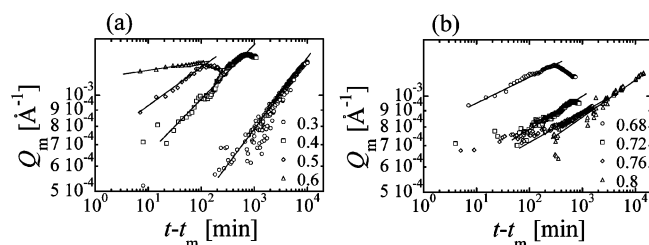


Figure 6. The peak positions Q_m are plotted against $t - t_m$ in double logarithmic form for $\phi_{\text{DMSO}} =$ (a) 0.3, 0.4, 0.5, 0.6 and (b) 0.68, 0.72, 0.76, 0.8. Solid lines represent the power law relation between Q_m and $t - t_m$.

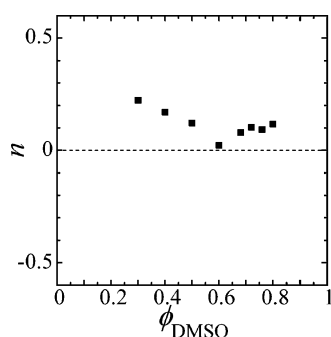


Figure 7. Solvent composition dependence of the exponent n in eq 3, which is estimated in Figure 6.

Figure 6a,b, the peak position Q_m is plotted against $t - t_m$ for various solvent compositions in a double logarithmic form. It was found for the PVA solutions in DMSO/water mixed solvents that the Q_m value increased with the annealing time ($t - t_m$) according to the power law, $Q_m \sim (t - t_m)^n$ (eq 3), for all the solvent compositions. For the solution with $\phi_{\text{DMSO}} = 0.6$, the peak position Q_m is almost independent of the annealing time, confirming that the SD-type phase separation occurs before cross-linking formation, as expected in the previous study,² although the slight increase in the peak position Q_m indicates that the degree of supercooling slightly increases with the progress of the cross-linking reaction. The exponent n was plotted against ϕ_{DMSO} in Figure 7. Note that the exponent evaluated here is not different from those in PIPS for epoxy resin formation,¹⁹ although the two systems are apparently very different, suggesting that the mechanism of molecular increase is essentially similar between the two systems. The exponent for $\phi_{\text{DMSO}} = 0.6$ is almost zero and increases toward both pure DMSO and water, showing that the supercooling is more effective below and above $\phi_{\text{DMSO}} = 0.6$. At a certain annealing time in the late stage, the peak position Q_m began to level off or decrease for $\phi_{\text{DMSO}} = 0.3, 0.4, 0.5, 0.68$, and 0.72 , although such a decrease in Q_m was not observed for $\phi_{\text{DMSO}} = 0.76$ and 0.8 . This suggests that the coalescence of the phase-separated domains is dominant in the late stage and the supercooling effect is negligible. It is noted that the upward shift of the phase diagram occurs effectively in the low molecular weight region of PVA, while the phase diagram does not move upward so much in the high molecular weight region. This is one of the reasons why the coalescence is effective for the decrease in Q_m in the late stage.

We also plotted the peak intensity against $t - t_m$ to find that it exponentially increases in the early stage, while it changes to a power law in the late stage, although the plot is not shown here. The exponential growth in the early stage may support an idea that the system comes into the SD region. The power law exponents in the late stage are rather large, depending on the solvent composition. The large value suggests that new small

domains are formed within the initially formed large domains during the annealing.

4. Conclusion

In the time-resolved light scattering measurements on the gelation process of PVA solutions in mixed solvent of DMSO and water, we found that a scattering peak characteristic of the SD phase separation appeared during the gelation process. For the PVA solution with the DMSO fraction $\phi_{\text{DMSO}} = 0.6$, which is the poorest solvent for PVA, the phase separation kinetic was almost described by the theory for normal isothermal SD-type phase separation, showing that the phase separation occurs almost before the cross-linking reactions among PVA chains. For other solvent compositions, on the other hand, the scattering peak appeared after a certain incubation time and the peak position moved to higher Q with the annealing time. The results contradict the theoretical prediction for normal isothermal SD-type phase separation. The results were explained in terms of gelation-induced phase separation.

When the PVA solution, which has UCST-type phase diagram, is quenched to the one-phase region, the phase separation, of course, does not occur. However, when the cross-linking reaction proceeds to increase the molecular weight, the phase diagram gradually shifts to the high-temperature side, and eventually, the PVA solution comes into the metastable region (or NG region). Further progress of the cross-linking reaction makes the phase diagram shift to the higher temperature side, and finally, the PVA solution enters the unstable region (or SD region). Then we observe a scattering peak characteristic of the SD-type phase separation in the light-scattering profile. After entering the SD region, the molecular weight further increases due to the cross-linking reaction, leading to the deeper quenching depth. This makes the peak position move to higher Q with annealing time. These GIPS phenomena were typically observed in the better solvent, because the phase diagram exists at a lower temperature than that for the poorest 60/40 solvent.

References and Notes

- (1) Kanaya, T.; Ohkura, M.; Takeshita, H.; Kaji, K.; Furusaka, M.; Yamaoka, H.; Wignall, G. D. *Macromolecules* **1995**, *28*, 3168–3174.
- (2) Takeshita, H.; Kanaya, T.; Nishida, H.; Kaji, K. *Macromolecules* **1999**, *32*, 7815–7819.
- (3) Takahashi, N.; Kanaya, T.; Nishida, K.; Takahashi, Y.; Arai, M. *Physica B* **2006**, *385–386*, 810–813.
- (4) Kanaya, T.; Ohkura, M.; Kaji, K.; Furusaka, M.; Misawa, M. *Macromolecules* **1994**, *27*, 5609–5615.
- (5) Kanaya, T.; Takeshita, H.; Nishikoji, Y.; Ohkura, M.; Nishida, K.; Kaji, K. *Supramol. Sci.* **1998**, *5*, 215–221.
- (6) Takeshita, H.; Kanaya, T.; Nishida, K.; Kaji, K.; Takahashi, T.; Hashimoto, M. *Phys. Rev.* **2000**, *E61*, 2125–2128.
- (7) Kanaya, T.; Takahashi, N.; Nishida, K.; Seto, H.; Nagao, M.; Takeda, T. *Phys. Rev.* **2005**, *E71*, 011801.
- (8) Takahashi, N.; Kanaya, T.; Nishida, K.; Kaji, K. *J. Appl. Polym. Sci.* **2005**, *95*, 157–160.
- (9) Ohkura, M.; Kanaya, T.; Kaji, K. *Polymer* **1992**, *33*, 3686–3690.
- (10) Ohkura, M.; Kanaya, T.; Kaji, K. *Polymer* **1992**, *33*, 5044–5048.
- (11) Takahashi, N.; Kanaya, T.; Nishida, K.; Kaji, K. *Polymer* **2003**, *44*, 4075–4078.
- (12) Chowdhury, A. H.; Russo, P. S. *J. Chem. Phys.* **1990**, *92*, 5744–5750.
- (13) Cahn, J. W.; Hilliard, J. E. *J. Chem. Phys.* **1958**, *28*, 258.
- (14) Cahn, J. W. *J. Chem. Phys.* **1965**, *42*, 93.
- (15) Cahn, J. W. *Acta Metall.* **1966**, *14*, 1685.

- (16) Both water and DMSO are respectively good solvent for PVA, while the mixture shows poor solvency for the polymer. This phenomenon is the so-called co-nonsolvency effect.
- (17) Bender, T. M.; Lewis, R. J.; Pecora, R. *Macromolecules* **1986**, *19*, 244–245.
- (18) Madbouly, S. A.; Ougizawa, T. *Macromol. Chem. Phys.* **2004**, *205*, 979–986.
- (19) Kyu, T.; Chiu, H.-W.; Lee, J.-H. In *Heterophase Network Polymers: Synthesis, Characterization and Properties*; Rozenberg, B. A., Sigalov, G. M., Eds.; Taylor & Francis: New York, 2002; Chapter 8, pp 91–106.
- (20) Yamanaka, K.; Takagi, Y.; Inoue, T. *Polymer* **1989**, *30*, 1839–1884.
- (21) Yamanaka, K.; Inoue, T. *Polymer* **1989**, *30*, 662–667.
- (22) Kim, B. S.; Chiba, T.; Inoue, T. *Polymer* **1993**, *34*, 2809–2815.
- (23) Kyu, T.; Lee, J. H. *Phys. Rev. Lett.* **1996**, *76*, 3746–3749.
- (24) Flory, P. J. In *Principles of Polymer Chemistry*; Cornell UP: Ithaca, NY, 1956.
- (25) Motoyama, M.; Yamazaki, Y.; Ohta, T. *J. Phys. Soc. Jpn.* **2001**, *70*, 729–732.
- (26) Aartsen, J. J. v. *Eur. Polym. J.* **1970**, *6*, 919–924.
- (27) Hashimoto, T.; Itakura, M.; Shimidzu, N. *J. Chem. Phys.* **1986**, *85*, 6773–6786.

MA071256T